The characterization, replication and testing of dermal denticles of *Scyliorhinus canicula* for physical mechanisms of biofouling prevention

2011 Bioinspir. Biomim. 6 046001

(http://iopscience.iop.org/1748-3190/6/4/046001)

Bioinsp. Biomim. **6** (2011) 046001 (11pp) doi:10.1088/1748-3182/6/4/046001

The characterization, replication and testing of dermal denticles of *Scyliorhinus canicula* for physical mechanisms of biofouling prevention

Timothy Sullivan and Fiona Regan

Marine and Environmental Sensing Technology Hub (MESTECH), National Centre for Sensor Research, School of Chemical Sciences, Dublin City University, Glasnevin, Dublin 9, Ireland

E-mail: fiona.regan@dcu.ie

Received 12 March 2011
Accepted for publication 15 August 2011
Published 12 October 2011
Online at stacks.iop.org/BB/6/046001

Abstract
There is a current need to develop novel non-toxic antifouling materials. The mechanisms utilized by marine organisms to prevent fouling of external surfaces are of interest in this regard. Biomimicry of these mechanisms and the ability to transfer the antifouling characteristics of these surfaces to artificial surfaces are a highly attractive prospect to those developing antifouling technologies. In order to achieve this, the mechanisms responsible for any antifouling ability must be elucidated from the study of the natural organism and the critical surface parameters responsible for fouling reduction. Dermal denticles of members of the shark family have been speculated to possess some natural, as yet unidentified antifouling mechanism related to the physical presence of denticles. In this study, the dermal denticles of one particular member of the slow-swimming sharks, *Scyliorhinus canicula* were characterized and it was found that a significant natural variation in denticle dimensions exists in this species. The degree of denticle surface contamination was quantified on denticles at various locations and it was determined that the degree of contamination of the dorsal surface of denticles varies with the position on the shark body. In addition, we successfully produced synthetic sharkskin samples using the real skin as a template. Testing of the produced synthetic skin in field conditions resulted in significant differences in material attachment on surfaces exhibiting denticles of different dimensions.

(Some figures in this article are in colour only in the electronic version)

1. Introduction

The adhesion of biological organisms to surfaces and the development of microbial multi-species communities (biofilms) has been a topical subject of research for several decades [1]. The formation of these communities has been implicated in antibiotic resistance and persistent bacterial infection such as those associated with cystic fibrosis [2, 3]. Biofouling, the growth of nuisance or unwanted biofilms on surfaces, is a major problem due to reduced efficiency, contamination and even failure of engineered components caused by such growth [4]. The economic costs of biofouling removal, combined with decreases in efficiency, performance, reliability, and increases in corrosion rates, have meant that many attempts have been made at producing surfaces that prevent or reduce the rate of biofouling accumulation [5]. Any means of removal, reduction, delay, or prevention of the process of biofouling, usually by the application of a coating containing biocides or by physical mechanisms, are referred to as antifouling coatings or antifouling strategies [6, 7].

1.1. Sharkskin and biomimetic design

Biomimetics, the creation of novel materials or engineering ideas inspired by the natural world, has been formally defined as the study of the structure and function of biological systems and processes as models of inspiration for the sustainable design and engineering of materials and machines [8]. The biomimetic design of novel antifouling materials is an attractive prospect, as many marine organisms appear to have an intrinsic natural ability to resist biofouling through non-toxic mechanisms [8]. Elasmobranchs, a subclass of cartilaginous fish that includes the sharks and rays of which there are some 1000 species [9], have been highlighted as a potentially rich source of bio-inspired design. Interest in this group from a biomimetic perspective began when early microscopic examination of the skin surface of the elasmobranchs showed that the skin surface was not smooth but instead featured microscopic placoid scales, which have been termed dermal denticles. Composed of dentine and enamel [10], these denticles are of a distinctive shape and precise orientation on the skin surface and are embedded in a deeper collagenous layer of the skin, the substratum compactum [11].

Investigation of possible advantages conferred on shark species by the presence of dermal denticles and particularly the work of Bechert [12, 13] led to detailed experiments on the nature and mechanism of hydrodynamic drag reduction by the presence of riblets on the dorsal surface of the denticles. Subsequent analysis of the drag reducing effects of mechanical riblets based on the structure of dermal denticle riblets indicated that the presence of riblets allowed certain fast-swimming shark species to gain an additional 8–10% swimming efficiency in comparison to a smooth surface. Attempts are underway to exploit this type of coating in various applications such as the Fastskin® body suit designed by Speedo as a drag reducing whole body swimsuit [14].

Dermal denticles are of interest in antifouling material development as it has been speculated that dermal denticles and riblets may possess dual functionality in both drag reduction and biofouling reduction [15]. However, inhibition of microbial adhesion by the presence of riblets or by the hydrodynamic conditions created by the presence of dermal denticles has not been proven experimentally. Shark dermal denticles have, however, recently inspired a successful commercial antifouling solution. Inspired by riblets on dermal denticles of fast swimming sharks, Sharklet AF™ is a novel antifouling solution that has proven to be effective in preventing the settlement of motile zoospores of the intertidal alga, *Ulva linza* [16, 17], and in controlling biofilm formation in *Staphylococcus aureus* [18]. Manufactured using a photolithographic process, Sharklet AF™ consists of a topographically textured surface with a repeating pattern of odd-numbered riblets of varying lengths. This mimics the pattern of riblets on real dermal denticles which usually consist of an odd number of riblets (3, 5 or occasionally 7 riblets). However, current manufacturing limitations mean that engineered surfaces such as Sharklet AF™ cannot match the topographic and dimensional complexity of real dermal denticles.

Testing the complexity of synthetic denticles with riblets for antifouling ability would be an attractive prospect. However, model surfaces used in generation of data for hydrodynamic flow analysis are prohibitively expensive, time consuming to produce and generally not suitable for field trials. Therefore, an inexpensive and repeatable method of generating synthetic sharkskin exhibiting dermal denticles is desirable. In this paper, we assess the use of real sharkskin from the catshark, *Scyliorhinus canicula,* as a template for producing inexpensive synthetic sharkskin exhibiting dermal denticles for antifouling testing. *S. canicula* was used in this study due to its widespread abundance, availability and as a representative member of the slow swimming sharks. Before preparing the synthetic template, a thorough characterization of the dermal denticles was carried out to gain information on the feature morphology and variation across the surface.

2. Experimental details

2.1. Reagents

We used poly(dimethylsiloxane) elastomer (PDMSe) (Sylgard 184 kit, Dow-Corning, Farnell, Ireland), Araldite epoxy resin kit (Epoxy resin kit R1030, Agar Scientific), ethanol (Cooley Distillery, Ireland), microscope slides (Corning), gluteraldehyde 25% v/v (Sigma-Aldrich), Petri dishes and 50 mL centrifuge tubes (Sarstedt, Ireland), trichloro(1H,1H,2H,2H-perfluorooctyl)silane (97% purity, Sigma-Aldrich) and silicone adhesive (Aquatics online).

2.2. Specimen collection

Specimens of *S. canicula* are captured as part of bycatch in lobster traps. Dead specimens were collected from fishing boats near Baltimore Harbour, County Cork, Ireland (51°29′ N; 09°22′ W). Several adult specimens approximately 660 mm in total length (TL) were collected, placed in a cool box and transported to the laboratory within 4 h, where measurements of total length were taken and skin samples of each were frozen to −18 °C to await further analysis. Samples for analysis of attached biofilm were prepared by fixation in gluteraldehyde (2.5% v/v) prior to removal to the laboratory and dehydrated in an ethanol series (30%, 50%, 70%, 80%, 90%, 95% v/v) once in the laboratory.

2.3. Sample preparation for electron microscopy

Skin samples, of area approximately 1 cm^2, were removed for microscopy with the aid of a scalpel. Care was taken to remove the surface gently from underlying tissues. Frozen skin samples were mounted on glass slides for examination by light microscopy. Skin samples for scanning electron microscopy (SEM) (Hitachi S3400N) were prepared for analysis by air drying samples at 20 °C for 1 h, before mounting on 15 mm Al stubs using double-sided adhesive carbon tabs and Au-sputter coating (Edwards 150 B coater). Imaging conditions typically included 10 mm working distance (WD), 5 keV accelerating voltage and probe current of 35 mA, samples were imaged in both secondary electron (SE) and backscattered

electron (BSE) modes. Comparison between air-dried and gluteraldehyde-fixed samples revealed little obvious difference in skin morphology if air-dried samples were imaged within several days of drying.

2.4. Measurement of dermal denticles

The dimensions of 150 dermal denticles were measured from four locations on the shark body using ImageJ software [19]. SEM images generated were imported into ImageJ and measurements were taken using the embedded scale bar from the SEM images. Measurements of maximum denticle length and width were taken directly using SEM software; denticles per mm^{-2} and the apical tip angle were measured in ImageJ. Percentage area estimation of contamination on the dorsal surface of individual denticles was also made using ImageJ.

2.5. Artificial skin preparation

Skin samples from four different peripheral areas of *S. canicula* for subsequent antifouling testing were replicated in two synthetic materials: embedding epoxy resin and poly(dimethylsiloxane) elastomer (PDMSe).

2.5.1. Master mould preparation. An initial master PDMSe mould was prepared from the skin of *S. canicula*. PDMSe was prepared by mixing ten parts by mass of poly(dimethylsiloxane) resin and one part by mass of the curing agent poly(methylsiloxane) as per manufacturer's instructions (Sylgard Kit 184, Dow Corning). The mixture was hand stirred for 2–4 min and then degassed under vacuum using a dessicator for 20–30 min to remove bubbles introduced during mixing. Approximately 10 cm^2 of frozen skin surface to a depth of 0.5–1 mm was removed using a sharp dissecting scalpel. Removed samples were gently rinsed in de-ionized water (18 Ω Milli-Q) and allowed to reach room temperature (18–25 °C). A vacuum (100 mbar for 30 min) was applied to the surface to remove excess water using a vacuum oven (Technico). To minimize distortion of the edges of the skin during this process, samples were placed onto glass microscope slides and the edges were sealed with clear varnish. Skin samples handled in this manner remained flat with minimal distortion when allowed to dry slowly at 20 °C for several days. Samples were then placed in clean Petri dishes and covered with mixed, degassed PDMSe to a depth of 4–5 mm. PDMSe of this depth was used in order to produce a mould of sufficient robustness to facilitate skin removal.

PDMSe was cured at 50 °C for 24 h and upon curing, skin samples were peeled away from the mould. It was found that the temperature and duration of curing of the PDMSe was sufficient to degrade the real skin surface, allowing the skin to be removed by flushing with water. On this occasion, isolated denticles remained embedded within the mould but were removed after casting of the first elastomer replicate.

2.5.2. Artificial skin production. An artificial skin was reproduced in PDMSe by silanizing the PDMSe master mould using trichloro(1H,1H,2H,2H-perfluorooctyl)silane. Master moulds were placed in a desiccator under vacuum with 10–20 μL of the silanizing agent for 40 min at 40 °C. Silanization is routinely used in microtechnology, and prevents bonding of a PDMSe surface to another PDMSe surface, thus facilitating the removal of cured elastomer from the mould. After silanization, moulds were filled with mixed and de-gassed PDMSe. Initial artificial skin surfaces produced were found to suffer from internal bubble formation as a result of gas entrapment in the original mould surface by curing PDMSe. To overcome this, it was found necessary to transfer the moulds and cure PDMSe through several vacuum cycles and massage the mould surface with a sterile rubber cell scraper to facilitate the release of entrapped gas from the surface. This technique resulted in bubble-free synthetic skin surfaces. PDMSe was then cured as described previously.

2.5.3. Epoxy resin skin production. Non-flexible artificial skin was also produced using epoxy resin; however, this surface was not assessed for effects on fouling. To produce artificial skin composed of epoxy resin, a kit designed for use as an SEM-embedding resin was used as per manufacturer's instructions (Araldite CY 212/DDSA/BDMA: 20/22/1.1 mL). The same protocol was followed as for the production of PDMSe replicas; however, curing of the epoxy resin occurred at 60 °C in a vacuum oven (Technico) at 200 mbar for 24 h.

2.6. Field testing of replicates

PDMSe artificial skin samples were assessed for antifouling ability in November 2010 at Lough Hyne Marine Reserve, Cork, Ireland (51°30′ N, 9°18′ W) (for a description of the Lough and associated research on the population of *S. canicula* present, see [20]). PDMSe skin samples ($n = 3$) from four separate body locations were mounted on glass microscope slides using acetic acid-based silicon adhesive. Prior to field trials, synthetic skin samples were conditioned in de-ionized water for 1 week to overcome any leaching acetic acid or other chemical contamination as a result of the production process. Smooth controls produced in PDMSe of the same thickness as the artificial skin samples underwent identical treatment. The slides with attached samples and controls were then mounted on a stainless steel backing panel and suspended in a high flow area with a mean flow of 3 m s^{-1} for 14 days at 1 m water depth. Other samples were suspended in an area of negligible flow for the same period. Samples in the high flow environment were securely anchored in order to keep samples orientated parallel to mean flow direction. Both sites had full light exposure, negligible freshwater input with little allochthonous material present in the water column. Samples were tested at depth of 1 m to ensure that light exposure was not a limiting factor and to minimize disturbance from wave action.

Upon completion of the field trial, samples were gently rinsed in clean seawater to remove any loosely attached contamination and preserved in gluteraldehyde (2.5% v/v) in 50 mL centrifuge tubes and transported back to the laboratory for analysis.

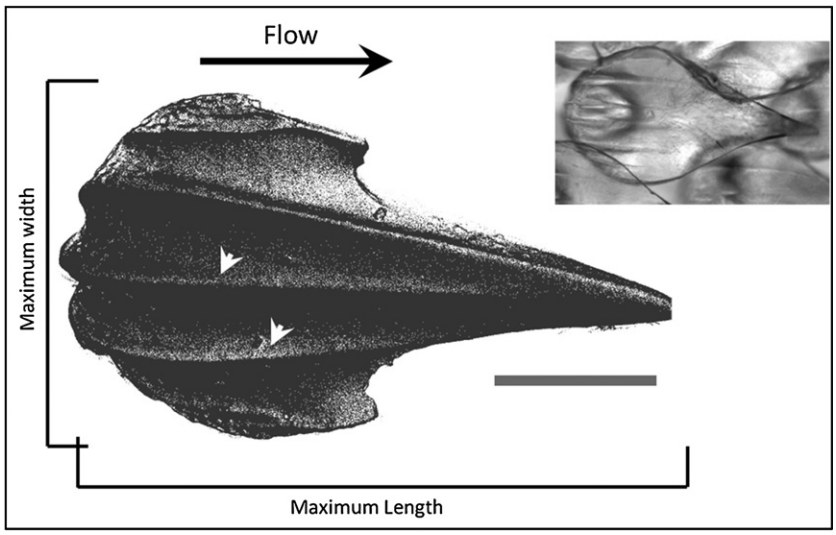

Figure 1. Illustration of the structure of the dorsal surface of a typical tridentate dermal denticle isolated from the skin of *S. canicula,* showing the surface riblets (arrowed) consisting of a central riblet with two flanking riblets converging at the denticle point. A light microscope image (inset) of a denticle shows the overlap between denticles on the skin surface. The number of riblets present on individual denticles varies but generally found in only odd numbers, usually 3, 5 or occasionally 7 (scale bar = 50 μm).

Table 1. Size variation of major characteristics of denticle shape with regard to location on the shark surface. Data taken from $n = 150$ denticles in each position except for denticle density/mm^2 where data were collected from $n = 36$ counts.

Skin location	Denticles/mm^2 $\pm$ SE ($n = 36$)	Mean maximum denticle length (μm) $\pm$ SE	Mean maximum denticle width (μm) $\pm$ SE	Ratio maximum length to width	Mean tip angle (deg) $\pm$ SE
Head	3.66 $\pm$ 1.33	729 $\pm$ 201	417.76 $\pm$ 92	1:1.8	27.8 $\pm$ 5.2
First dorsal fin	7.66 $\pm$ 1.46	470.8 $\pm$ 77.4	320.2 $\pm$ 41	1:1.5	39.7 $\pm$ 8.4
Second dorsal fin	19.2 $\pm$ 2	336.3 $\pm$ 36.5	233.8 $\pm$ 21	1:1.4	61.5 $\pm$ 6.7
Caudal fin	17.28 $\pm$ 2.61	332.8 $\pm$ 40.5	244 $\pm$ 32.6	1:1.4	59.1 $\pm$ 9.3

2.7. Fouling assessment

The degree of fouling was assessed by measuring the percentage increase in total mass on each of the samples. The degree of microfouling and sedimentation between denticles was examined by thin sectioning the replicates using a scalpel blade and imaging with SEM as described previously. Attached biofouling organisms were identified using SEM and light microscopy.

2.8. Data analysis methods

Differences in the total mass change among replicates ($n = 12$) of synthetic sharkskin produced from locations on the body of *S. canicula* were compared by one-way analysis of variance (ANOVA) with body location as a fixed factor. Differences between locations were then compared using Tukey's *post hoc* HSD tests.

3. Results and discussion

3.1. Denticle characterization

Microscopic examination and measurement of the dermal denticles of *S. canicula* revealed variation in both denticle shape and dimensions, depending upon the location on the body of the shark. While retaining the tridentate shape reported in the literature [10], denticles were generally more elongated than typically reported with less pronunciation of the riblets on the dorsal surface of the denticle (figure 1). The measurement of maximum dimensions at different points on the body revealed a progressive change in the ratio of length to width, showing greater elongation of denticles towards the head of *S. canicula* and a corresponding change in the overall shape of the denticles (figure 2). A progressive reduction in the total denticle size was measured from the head to the caudal fin (figure 3). Physical manipulation of the denticles revealed some degree of scale bristling also reported by Lang *et al* [11]; however, this was not examined further. Table 1 provides a summary of denticle dimensions from the selected locations on a shark body (overall specimen length = 660 mm).

3.2. Quantification of denticle surface contamination

Although there is some evidence of the production of chemical antimicrobials in sharks [21], the mechanisms by which sharks prevent fouling or epibiosis remain unclear. No analysis of the extent to which the denticles of *S. canicula* become colonized by microbial organisms have been published to the author's knowledge, although it has been suggested that this species is susceptible to dermal parasitic infestation in Irish waters [22].

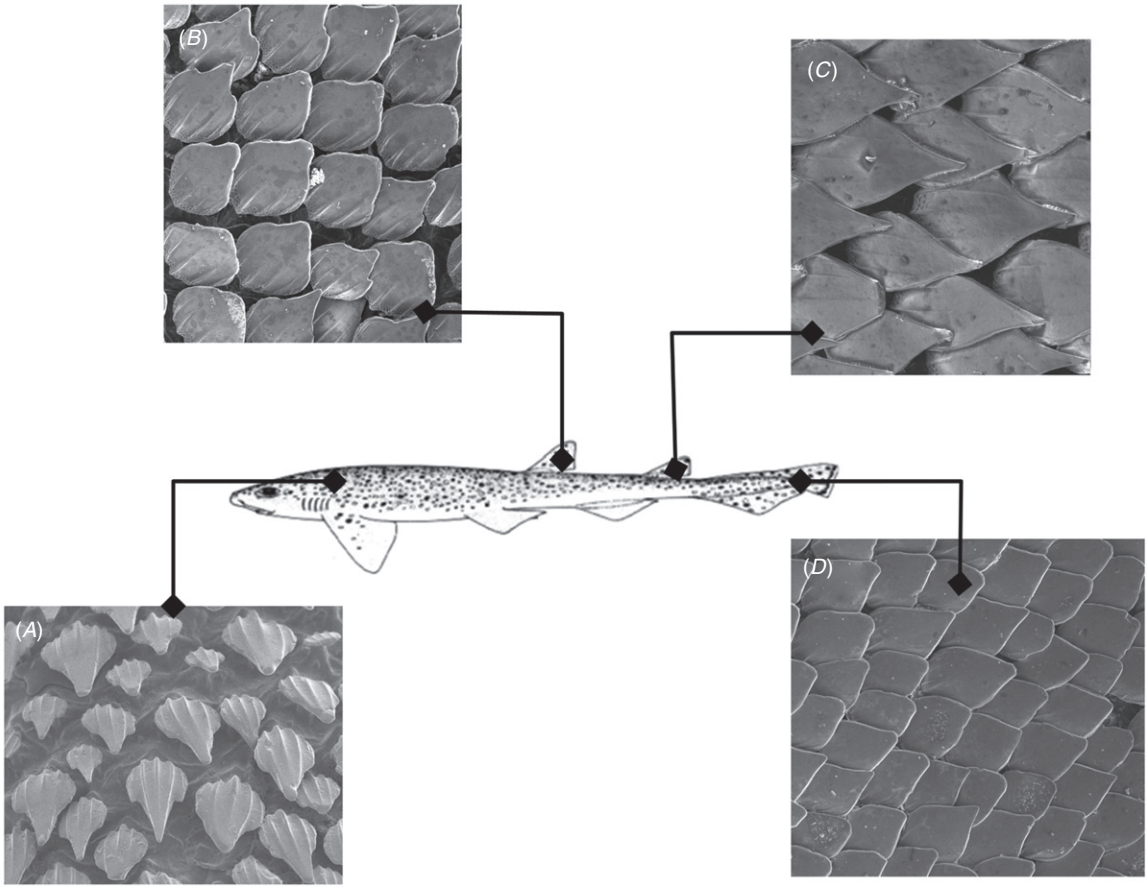

Figure 2. SEM images illustrating the variation in dermal denticle shape across the body surface of *S. canicula*, showing gradual variation from a large three-pointed denticle to a teardrop-shaped denticle with an elongated terminal point (*A*) through to shortened denticles with a large overlap (*D*) with large variation at intermediate stages.

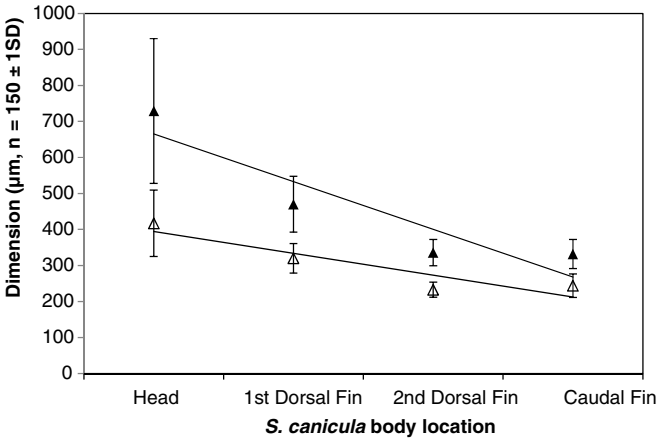

Figure 3. Variation in overall dimensions of dermal denticle length (filled triangles) and width (open triangles) with respect to location on the surface of *S. canicula*; correlation between the location of the shark surface and maximum denticle length ($r^2 = 0.84$) and maximum width ($r^2 = 0.8475$) is seen on skin samples when measured from head to caudal fin on the shark body.

The ability of the egg case of *S. canicula* to inhibit fouling has been attributed to heavy metal scavenging or a Fenton-like reaction on the outer surface [23, 24]. However, such mechanisms appear unlikely on dermal denticles given their composition.

In this study, microscopic examination of denticle surfaces was carried out using SEM. The images revealed limited bacterial colonization of isolated denticles; however, no diatom frustules were seen. Quantification of biofilm growth by methods such as crystal violet staining or carbohydrate and protein analysis was not reliable due to the complex topographic nature of the skin surface. The latter were also of limited use due to the use of dried samples. Therefore, quantification of contamination of the dorsal surface of individual denticles was carried out by the study of the SEM images. Calculation of the contaminated area as a percentage of the total denticle surface area was carried out ($n = 10$ randomly selected denticles from each location). While individual bacterial colonies were observed on the denticle surface, not all contamination could be identified as microbial in origin and may have included mucilage secretions from the skin surface; hence, percentage contamination is used only as an estimate of possible microbial fouling of the denticle surface. It was found that denticles from skin samples on the head and caudal fin areas exhibited less surface contamination, as illustrated in figure 4.

Furthermore, increases in denticle contamination were observed in close proximity to the skin surface with

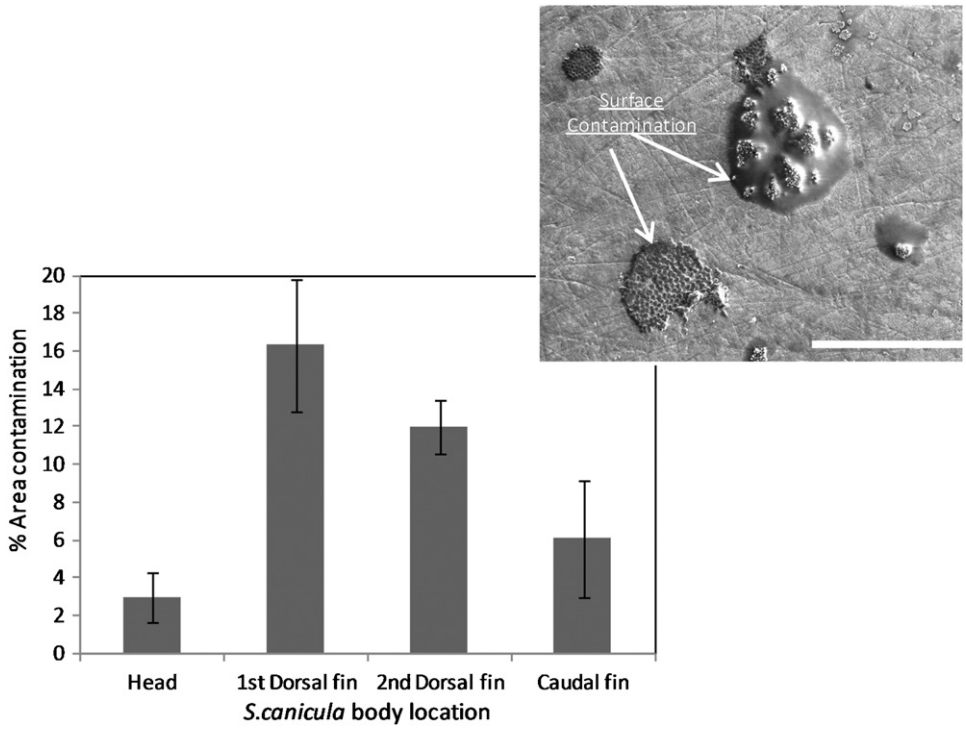

Figure 4. Contamination of the dorsal surface of dermal denticle sampled from locations on the body surface of *S. canicula* as estimated by measuring the contamination of the denticle surface as a percentage of the total denticle surface area. Inset micrograph indicates surface contamination as visualized by SEM (scale bar = 50 μm).

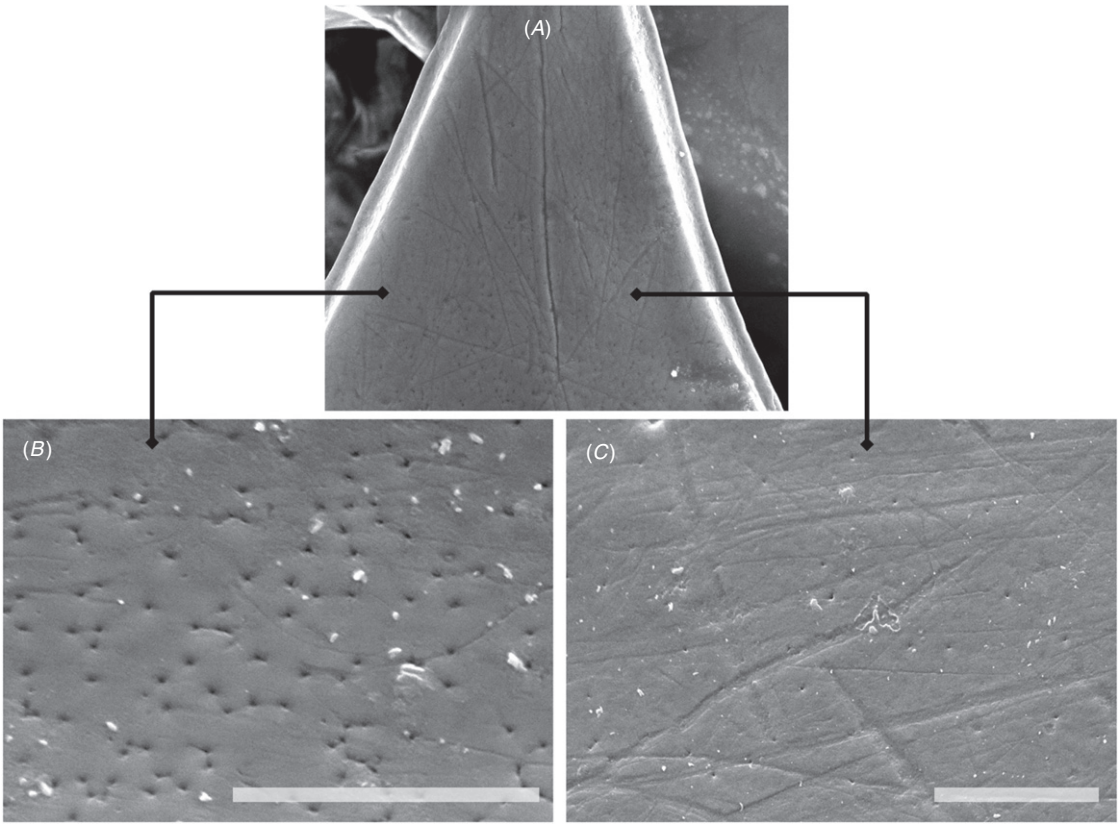

Figure 5. SEM illustration of the tip of an isolated dermal denticle of *S. canicula* and enlarged detail of the microtopographic detail on the denticle surface showing surface pitting (*B*) and linear surface scratches (*C*), possibly formed as a result of mechanical abrasion through denticle contact with other sharks or contact with sand or other surfaces (scale bar = 20 μm).

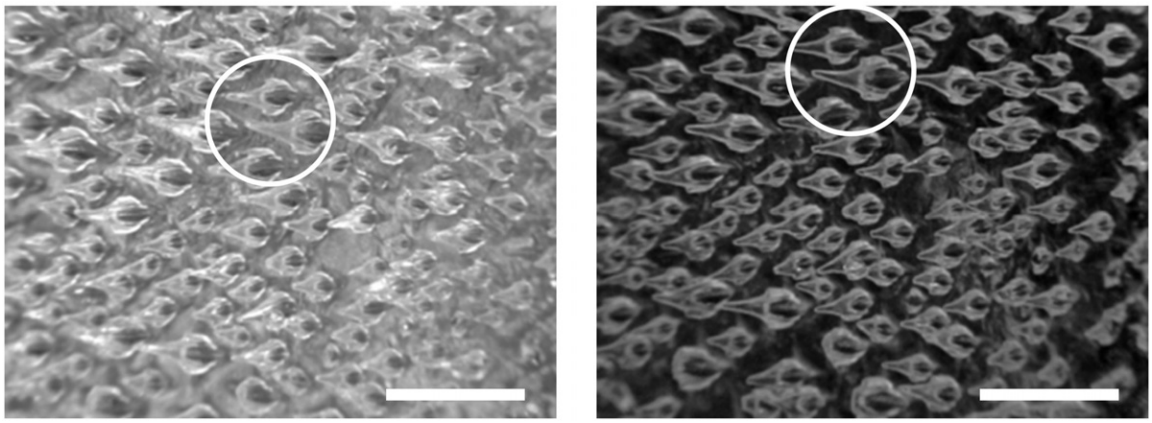

Figure 6. USB digital microscope image (magnification ×400) of a skin sample containing dermal denticles taken from the head of *S. canicula* (left) and epoxy resin replicate of the same surface (right); the circled area represents the same dermal denticle as imaged on both surfaces (scale bar ≈ 500 μm).

contamination being less prevalent towards the tip of the denticles, a fact that may be related to the increased shear forces associated with the protrusion of the denticle tip into the laminar flow layer unaffected by the skin surface.

3.3. Denticle microstructure

Examination of the microtopography of the surface of individual denticles revealed the presence of surface scratches (figure 5), the majority of which were roughly parallel with the longitudinal axis of the denticle. These features appear consistent with mechanical abrasion from contact with sand or rock on the seafloor or perhaps from behavioural characteristics of the shark such as refuging behaviour or contact with other denticles during feeding behaviour [25]. The presence of such surface scratches may indicate that mechanical abrasion of the denticle surface may have some role in fouling removal, although behaviour indicative of this has not been recorded in *S. canicula*. It has also been speculated that specific microtopography of marine organisms may have some function in preventing the adhesion of fouling organisms [26], particularly with regard to periodic linear features which may reduce the binding energy between the surface and adhering cells and related to the number of attachment points, as summarized in the attachment point theory of antifouling surfaces based on surface topography [27, 28]. However, the lack of consistent waviness, isotropy, or other continuity in the microtopographic structure does not support the view that microbial adhesion is prevented by surface micro-texture in *S. canicula*. Pit-like structures are seen on isolated denticles; however, no attempt was made to characterize the function of these surface features.

3.4. Synthetic skin production

This paper reports the first synthetic replication of complete physical dermal characteristics of *S. canicula*. The described technique for producing synthetic skin samples exhibiting dermal denticles uses the real skin as a master mould. Similar techniques to that described are routinely used in micro-fluidics to generate topographically complex structures [29]. A similar technique has been used to successfully create replicas of the surface structure of lotus leaves [30]. When cured, PDMSe retains accuracy of features of 20 nm in dimension [31], which is more than adequate for accurate reproduction of the main topographic features of dermal denticles. Skin features were also successfully reproduced in epoxy resin using the PDMSe master mould created (figure 6). The use of PDMSe to create synthetic skin surfaces from the master mould resulted in surfaces that could be readily tested for antifouling ability, yielding exact replicas of larger denticles that did not widely overlap. The attachment base and ventral surface of dermal denticles reproduced on synthetic skin surfaces from areas of skin containing widely spaced denticles were also accurate (figure 7).

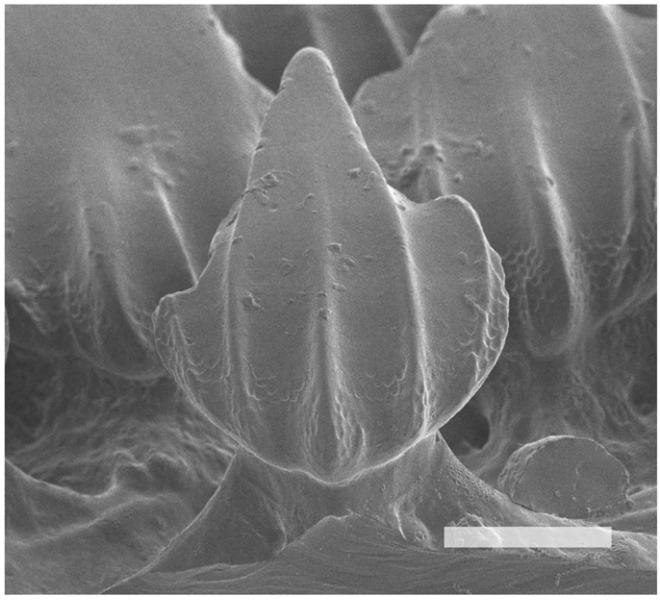

Figure 7. SEM image of a synthetic dermal denticle reproduced in PDMSe. Riblets are faithfully reproduced on the elastomeric denticle surface, as are areas of surface contamination present on the dorsal surface of the original dermal denticle (scale bar = 200 μm).

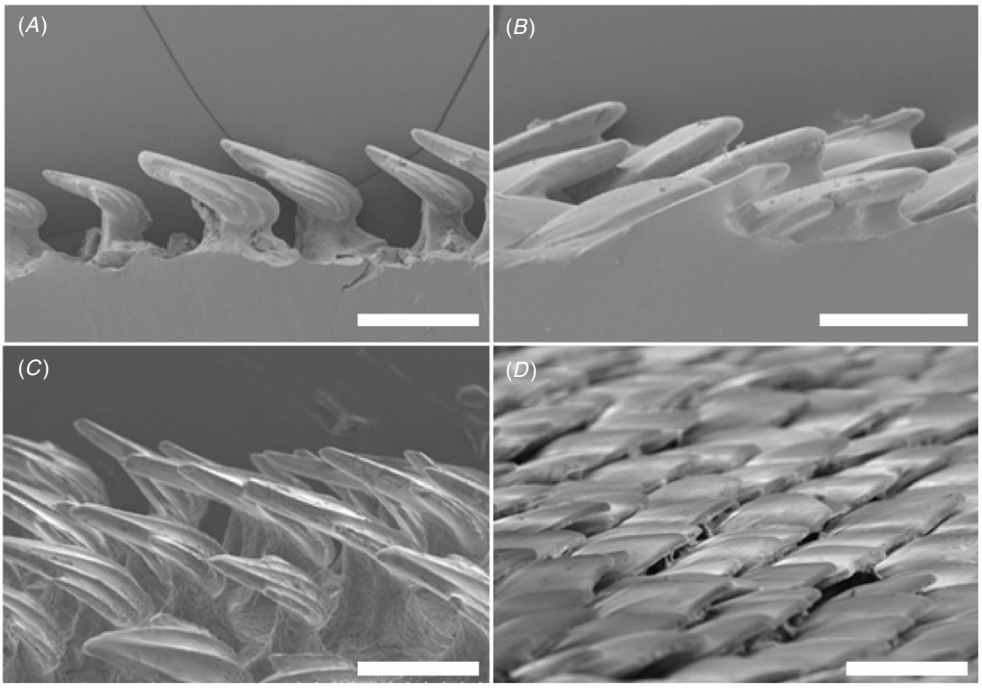

Figure 8. SEM cross-section of dermal denticles at the first dorsal fin of *S. canicula* showing synthetic PDMSe denticles (*A*) and real surface (*C*). Synthetic dermal denticles reproduced from the caudal fin of *S. canicula* are shown in (*B*) with the real surface (*D*). PDMSe replication of dermal denticles with larger spacing and less overlap between denticles was accurate; however, for locations with larger areas of individual denticle overlap and with smaller denticles, PDMSe replicas of the surface were less accurate possibly as a result of insufficient penetration of the PDMSe into the spaces between the underlying skin surface and the denticle (scale bar = 100 μm).

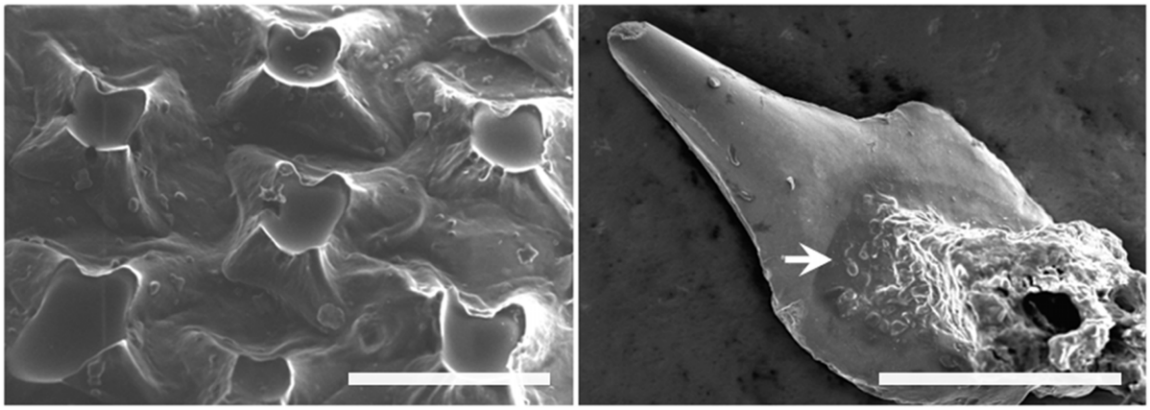

Figure 9. Illustration of the attachment mechanisms of dermal denticles to the underlying skin surface in *S. canicula*; (*a*) epoxy resin replicate denticle basal support structure prepared as described and (*b*) the ventral surface of an actual isolated denticle showing the extent of the attachment base and central cavity and unicellular gland cells present, arrowed (scale bar = 200 μm).

Acceptable replicas of the dorsal surfaces of smaller, densely packed, overlapping denticles found on the caudal and second dorsal fins were also produced with retained features. However, the ventral surface and denticle support structure and attachment points were not fully reproduced. This is likely due to failure of the PDMSe to properly infiltrate the recesses beneath the denticles as indicated by microscopic examination of cross sections of the synthetic skin taken in these locations (figure 8).

Denticle attachment points to the skin surface at each location could be observed by producing replicas without degassing of the PDMSe from the mould. This allowed gas bubbles to remain entrapped in the mould in the voids produced by the dermal denticles, preventing the replication of the denticle, yet producing a good replica of the denticle attachment base on the skin surface (figure 9).

3.5. Assessment of fouling of synthetic sharkskin

Standard methods of biofouling quantification by spectroscopic or biochemical methods are generally not suitable for the assessment of fouling on topographically rough surfaces. In view of this, a combination of total mass increase, coupled with SEM visualization, was used to give an

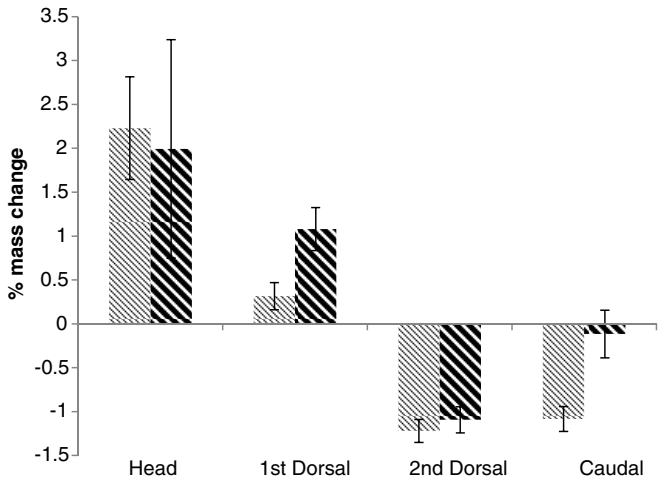

Figure 10. Graph of the percentage change in total mass of synthetic sharkskin produced from different locations on the body of *S. canicula* after exposure in fouling conditions for 14 days. Data have been normalized to mass change of smooth PDMSe surfaces of the same planar area. Changes for both high flow (light cross-hatching) and low flow (heavy cross-hatching) regimes are shown. Synthetic skin samples produced from body locations exhibiting smaller dermal denticles show a reduction in total mass change after a period of 14 days compared to a corresponding smooth surface.

indication of the effects of the presence of dermal denticles on the degree, location and nature of fouling present after the 14 day study.

Differences were measured in the total mass increase on replicas taken at various locations on the surface of the shark when subjected to different fouling environments (figure 10). Synthetic skin samples reproduced from all locations on the shark surface showed increases in the total mass compared to a smooth PDMSe control surface of the same planar surface area when exposed in a low flow environment. Areas of synthetic skin with fewer, larger, denticles showed larger mass increases compared with synthetic skin with a higher density of denticles, albeit with a reduction in the mean size.

Thin sections through fouled synthetic skin examined using SEM revealed a propensity for skin surfaces with larger denticles to accumulate greater sedimentation, a fact that may be attributed to the isolated nature of individual denticles entrapping sedimentation close to the skin surface. The smaller denticle sizes together with a larger degree of overlap on dorsal and caudal surfaces may prevent accumulation of sediment and explain the smaller increase in mass measured on these surfaces. In addition, the greater overall denticle size and lower denticle density allowed greater diatom and bacterial attachment possibly due to light penetration and protection from shear forces (figure 11), especially for the common benthic diatom genus, *Cocconeis,* which could be seen to attach to the undersides of the denticles in such locations.

Synthetic skin exposed in a high energy fouling environment exhibited the same overall trend as samples exposed in the low energy environment. It was found that there was a greater total mass increase on surfaces with larger

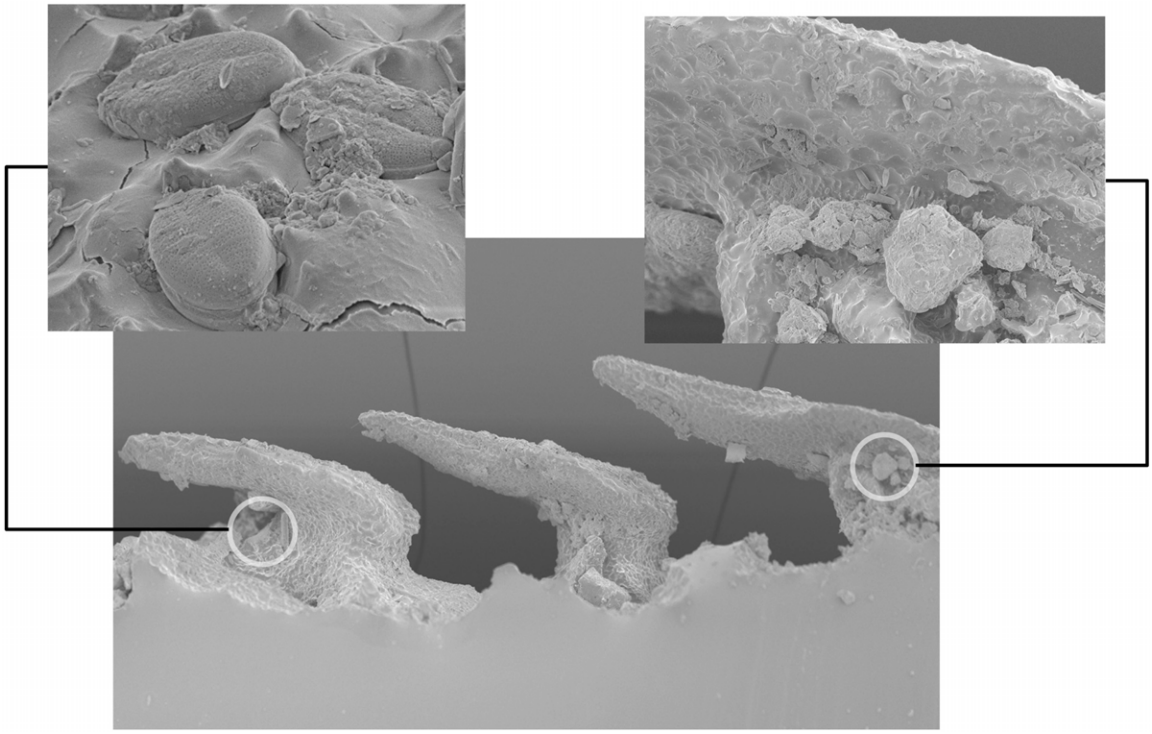

Figure 11. A thin section through a sample of synthetic sharkskin produced from the head of *S. canicula*, as observed using SEM. The sample has been exposed to a low hydrodynamic flow fouling environment for a period of 14 days. Attachment of diatom frustules and particulate sedimentation between PDMS dermal denticles can be observed, indicating a possible source of the increases in total mass seen in synthetic skin samples from this location.

Table 2. ANOVA of mass difference.

Mass change	Sum of squares	df	Mean square	F	Significance
Between groups	36.243	3	12.081	8.089	0.001
Within groups	29.871	20	1.494		
Total	66.114	23			

denticles and less denticle interlocking as seen at the head and first dorsal fin locations. This result is supported by the results of the one-way ANOVA analysis (F (3, 20) = 8.089, $p = 0.001$) (table 2) illustrating a significant difference based on location. Tukey's HSD *post hoc* comparisons among the synthetic skin replicates indicate that synthetic skin from the head ($M = 4.68$, 95% CI [3.38, 5.99] developed significantly greater mass than that of synthetic skin from all other areas; there was no significant difference between replicates from the first dorsal fin ($M = 2.64$, 95% CI [2.64, 3.53]), second dorsal ($M = 1.44$, 95% CI [0.26, 2.6]) or caudal fins ($M = 1.97$, 95% CI [0.33, 3.6]). However, increases in total mass when exposed at high flow locations were less than those experienced by a smooth surface under the same conditions, indicating that denticle configuration and spacing may have a role either in increased fouling release or perhaps reduced adhesion of contamination and biofouling. This is an exciting result as it had been anticipated that surfaces containing dermal denticles and thus having a larger overall surface area for fouling would show increases in mass compared to a smooth surface with the same planar area. From the literature, there is some evidence to suggest that the distinct shape of the denticles may alter the depth of the boundary layer close to the denticle surface resulting in the formation of primary and secondary vortices [11]. This may influence the ability of potential fouling propagules or sedimentation to contact or attach to the denticle surface. Recent studies have shown that micro-geometry of surfaces can considerably influence the rate and strength of adhesion of fouling organisms [32, 33], and in this study a number of diatom species could be seen to attach within surface cavities, possibly due to the protection afforded to the cells from shear forces.

4. Conclusions

In this work, the use of real sharkskin from the catshark, *S. canicula* was assessed for the first time as a template for producing inexpensive synthetic sharkskin exhibiting dermal denticles for field assessment of fouling. The real skin surface containing dermal denticles exhibited considerable natural variation in denticle morphology, depending upon the position on the body of the shark. Field testing of fouling accumulation on synthetic skin from areas of differing dermal denticle dimensions illustrated small but significant differences in contamination rates between synthetic skin samples. Smaller, densely packed denticles resulted in a reduction in contamination when compared to a smooth elastomer surface of identical planar surface area. This suggests that sharkskin dermal denticles may possess a dual functionality in both drag reduction and reduction of surface fouling. Further investigation into the effects of hydrodynamic conditions created by the presence of dermal denticles on biofouling propagule adhesion at the skin surface is required.

Acknowledgments

The authors would like to gratefully acknowledge funding from the Beaufort Marine Research Awards, carried out under the *Sea Change Strategy* and the Strategy for Science Technology and Innovation (2006–2013), with the support of the Irish Marine Institute, funded under the Marine Research Sub-Programme of the National Development Plan 2007–2013. Thanks are due to Dr Rob McAllen and Professor John Davenport of University College Cork and Patrick Graham and Declan O'Donnell from the National Parks and Wildlife Service of Ireland for access to Lough Hyne Marine Reserve (Research permit no R36-38/10). They also thank the School of Chemical Sciences and acknowledge DCU technical support from Brendan Twamley for the use of SEM.

References

[1] Costerton J W, Lewandowski Z, Caldwell D E, Korber D R and Lappin-Scott H M 1995 Microbial biofilms *Annu. Rev. Microbiol.* **49** 711–45
[2] Costerton J W, Stewart P S and Greenberg E P 1999 Bacterial biofilms: a common cause of persistent infections *Science* **284** 1318–22
[3] Stewart P S and William C J 2001 Antibiotic resistance of bacteria in biofilms *Lancet* **358** 135–8
[4] Flemming H C, Murthy P S and Venkatesan R 2009 *Marine and Industrial Biofouling* (Berlin: Springer))
[5] Callow M E and Callow J E 2002 Marine biofouling: a sticky problem *Biologist* **49** 1–5
[6] Almeida E, Diamantino T C and de Sousa O 2007 Marine paints: the particular case of antifouling paints *Prog. Org. Coat.* **59** 2–20
[7] Whelan A and Regan F 2006 Antifouling strategies for marine and riverine sensors *J. Environ. Monit.* **8** 880–6
[8] Salta M *et al* 2010 Designing biomimetic antifouling surfaces *Phil. Trans. R. Soc.* A **368** 4729–54
[9] Musick J A, Burgess G, Cailliet G, Camhi M and Fordham S 2000 Management of sharks and their relatives (Elasmobranchii) *Fisheries* **25** 9–13
[10] Hamlett W C 1999 *Sharks, Skates, and Rays: The Biology of Elasmobranch Fishes* (Baltimore, MD: Johns Hopkins University Press)
[11] Lang A W, Motta P, Hidalgo P and Westcott M 2008 Bristled shark skin: a microgeometry for boundary layer control? *Bioinsp. Biomim.* **3** 046005
[12] Bechert D W, Bartenwerfer M, Hoppe G and Reif W E 1986 Drag reduction mechanisms derived from shark skin *Proc. 15th ICAS Congress (London, 7–12 September 1986)* vol 2 (A86-48976 24-01) (New York: American Institute of Aeronautics and Astronautics, Inc.) pp 1044–68
[13] Bechert D W, Hoppe G and Reif W E 1985 On the drag reduction of the shark skin *AIAA Shear Flow Control Conf.*
[14] Bhushan B 2009 Biomimetics: lessons from nature—an overview *Phil. Trans. R. Soc.* A **367** 1445–86
[15] Bechert D W, Bruse M, Hage W and Meyer R 2000 Fluid mechanics of biological surfaces and their technological application *Naturwissenschaften* **87** 157–71

[16] Schumacher J F *et al* 2007 Engineered antifouling microtopographies—effect of feature size, geometry, and roughness on settlement of zoospores of the green alga Ulva *Biofouling* **23** 55–62
[17] Schumacher J F *et al* 2007 Species-specific engineered antifouling topographies: correlations between the settlement of algal zoospores and barnacle cyprids *Biofouling* **23** 307–17
[18] Chung K K, Schumacher J F, Sampson E M, Burne R A, Antonelli P J and Brennan A B 2007 Impact of engineered surface microtopography on biofilm formation of *Staphylococcus aureus Biointerphases* **2** 89–95
[19] Rasband W S 1997–2011 *ImageJ* (Bethesda, MD: National Institutes of Health) (http://imagej.nih.gov/ij/)
[20] Sims D, Nash J and Morritt D 2001 Movements and activity of male and female dogfish in a tidal sea lough: alternative behavioural strategies and apparent sexual segregation *Mar. Biol.* **139** 1165–75
[21] Moore K S *et al* 1993 Squalamine: an aminosterol antibiotic from the shark *Proc. Natl Acad. Sci. USA* **90** 1354–8
[22] Henderson A C and Dunne J J 1998 The metazoan parasites of the lesser-spotted dogfish *Scyliorhinus canicula* (L.) from the Galway Bay area *Ir. Nat. J.* **26** 104–7
[23] Thomason J C, Davenport J and Rogerson A 1994 Antifouling performance of the embryo and eggcase of the dogfish *Scyliorhinus canicula J. Mar. Biol. Assoc.* **74** 823–36
[24] Thomason J C, Marrs S J and Davenport J 1996 Antibacterial and antisettlement activity of the dogfish (*Scyliorhinus canicula*) eggcase *J. Mar. Biol. Assoc.* **76** 777–92
[25] Southall E J and Sims D W 2003 Shark skin: a function in feeding *Proc. R. Soc. (Suppl. 1)* B **270** S47–9
[26] Bers A V and Wahl M 2004 The influence of natural surface microtopographies on fouling *Biofouling* **20** 43–51
[27] Scardino A, Harvey E and De Nys R 2006 Testing attachment point theory: diatom attachment on microtextured polyimide biomimics *Biofouling* **22** 55–60
[28] Scardino A 2008 Attachment point theory revisited: the fouling response to a microtextured matrix *Biofouling* **24** 45–53
[29] Anderson J R *et al* 2000 Fabrication of topologically complex three-dimensional microfluidic systems in PDMS by rapid prototyping *Anal. Chem.* **72** 3158–64
[30] Sun M *et al* 2005 Artificial lotus leaf by nanocasting *Langmuir* **21** 8978–81
[31] Zhao X M, Xia Y and Whitesides G M 1997 Soft lithographic methods for nano-fabrication *J. Mater. Chem.* **7** 1069–74
[32] Scardino A J, Hudleston D, Peng Z, Paul N A and de Nys R 2009 Biomimetic characterisation of key surface parameters for the development of fouling resistant materials *Biofouling* **25** 83–93
[33] Bersa A V *et al* 2010 Relevance of mytilid shell microtopographies for fouling defence—a global comparison *Biofouling* **26** 367–77